Influence of the remnant magnetization, size distribution and content of soft magnetic reinforcement in micro-mechanical behavior of polymer matrix composites

G. Riesgo[1], L. Elbaile[2], R. Moriche[4*], J. Carrizo[2], R. D. Crespo[2], M.A. García[3], R. Sepúlveda[4], J.A. García[2] and Y. Torres[4]
[1] Centro de Seguridad Marítima Integral Jovellanos, Camín del Centro de Salvamento nº 279. 33393 Gijón. Spain
[2] Dpto. de Física de la Universidad de Oviedo, c/ Calvo Sotelo s/n, 33007 Oviedo, Spain.
[3] Dpto. de Ciencia de los Materiales. Universidad de Oviedo, c/ Independencia nº 13, 33004 Oviedo, Spain.
[4] Dpto. de Ingeniería y Ciencia de los Materiales y el Transporte, Universidad de Sevilla, Sevilla, Spain
* Corresponding author (rmoriche@us.es)

Abstract

In this work, the influence of the remnant magnetization, size distribution and content of soft magnetic reinforcement in micro-mechanical behavior of polymer matrix composites ($Fe_{81}Ga_{19}$/silicone) are evaluated. Melt spinning ribbons were pulverized in a planetary milling machine to act as composite particle reinforcement. The instrumented microindentation behavior (Young´s modulus and Vickers micro-hardness), the pseudo-creep and relaxation phenomena as a function of the microstructure have been studied. In general, the micro-hardness, stiffness and elastic recovery of the studied composite materials increased with the filler content. Magnetic saturation did not change with the milling technique, and composite remnant magnetization increased with either contend or particle size. Additionally, the magnetization process improved the Vickers micro-hardness and Young's modulus of composites. Finally, pseudo-creep and stress relaxation behavior was also dependent on $Fe_{81}Ga_{19}$ content and size distribution.

Keywords: Polymer-matrix composite; Magnetic properties; Mechanical properties; Stress relaxation; Pseudo-creep

1. Introduction

Nowadays, many technical applications require materials whose properties cannot be obtained by conventional manufacturing processes. To accomplish this fact, materials that merge many different properties are necessary. That is the case of magneto-active composite materials [1-3], where mechanical properties of elastomeric materials are combined with a magnetic response due to the integration of magnetics particles within. Those materials constitute a new class of smart materials that change their mechanical properties under the application of a magnetic field [4-6], having strong possibilities of being applied in different technical applications, especially for active stiffness and vibration control of structured systems [7-8] and in aircraft applications [9]. The mechanical behavior of magneto-active composites materials is determined by the elastic properties of the matrix and the magnetic properties of the particles [10]. Recently, the magnetostriction in FeAl/polyester and FeAl/ silicone composites was studied [11], and the obtained results could open the possibility of using these materials in the sensor technology field.

The magnetorheological elastomers materials (MRES) can be divided in: a) anisotropic, cured under the presence of a magnetic field, so particles are aligned in chain-like structures; and b) isotropic (also call elastomer-ferromagnet composites), cured in the absence of any magnetic field, so particles result randomly distributed within the matrix [12]. Thus, mechanical deformation driven by a magnetic field performs differently on each case. Theoretical studies performed by Borcea et al. [13] predict an expansion along the applied magnetic field in the isotropic materials and a compression in the anisotropic ones.

The mechanical response of MRES to an applied magnetic field is basically influenced by the nature of the filler particles and its alignment degree. In conventional MRES, soft

magnetic particles, mainly iron particles, have been used to obtain the maximum change in the mechanical properties under the action of the applied magnetic field [14, 15]. Just recently, a new kind of magnetorheological elastomers have been manufactured with hard magnetic particles [16-19]. These composite materials have shown a non-elastic behavior even without any applied magnetic field, and their Young`s modulus seems to be strain dependent, both characteristics are attributed to the use of high remnant magnetization particles. In fact, when the magnetorheological elastomer is anisotropic, magnetic poles are formed and composite materials perform similar to a flexible magnet.

In this article, we present a magnetorheological elastomer made with $Fe_{81}Ga_{19}$ soft magnetic particles, obtained by melt spinning, embedded in a liquid silicone matrix. The micro-mechanical behavior (Young´s modulus and *Vicker* micro-hardness), the pseudo-creep and relaxation phenomena as a function of the weight fraction and size of the reinforcement particles have been studied. In spite of the fact that the reinforcement particles have a soft magnetic behavior, an influence of the magnetization of the magnetorheological elastomer has been observed and studied.

2. Experimental procedure

High purity (99.9 %) Fe and Ga metals were used as raw materials. Alloys ingots of $Fe_{81}Ga_{19}$ were prepared by induction melting under vacuum atmosphere. From these ingots, ribbons of about 2 mm wide and 60 µm thick were produced by planar flow casting in vacuum atmosphere with a roll speed of 17.5 m/s.

A mass of 25 g of manually cropped ribbons of $Fe_{81}Ga_{19}$ were milled under vacuum atmosphere using a planetary ball mill (Retsch, PM 100 model). A 500 ml 1.2080 tool steel jar with 20 tempered steel balls of 10 mm in diameter were used as a milled

container, setting a ball to powder ratio of 40:1 with a rotational speed of 400 rpm. To reduce further powder contamination, no lubrication or process control agents were added. The milling process lasted 2 h and it was interrupted every 20 min to dissipate the accumulated heat. In order to trace the evolution on the particle size, during each milling interruption, particles were sieved using ASTM E-11/95 sieves, weighted and carefully returned to the jar to restart the milling. At the end, 4 different groups of particle sizes (under 50 μm, 150-180 μm, 180-250 μm, and above 250 μm) were made. The magnetic characterization of the $Fe_{81}Ga_{19}$ particles was carried out at room temperature using a vibrating sample magnetometer (EV9 – VSM 2.2 T) with the aim of elucidating their magnetic parameters. The metallic reinforcement was previously sieved and classified in different size distribution ranges. Once classified, polymer matrix composites were manufactured using (Silicone Ceys Ms-Tech) with: 1) different reinforcement contents (particles size <50 μm) and 2) different size distributions ($Fe_{81}Ga_{19}$ content of 60 wt%). Table 1 shows $Fe_{81}Ga_{19}$/Silicone composite materials analyzed in this work. The composites were prepared by dispersing the powders into the silicone matrix following the next procedure: all the components were mixed with a stirrer bar at room temperature and the mixture was put into a prism shape mold with dimensions of 50 mm × 30 mm and thickness of 10 mm.

Table 1. Experimental matrix of the composites investigated.

	Particles size (μm)	**Reinforcement content**	
		Weight fraction (wt%)	**Volume fraction (vol%)**
Silicone	-	0	0
Influence of reinforcement content	< 50	50	12.4
		60	17.5
		70	24.8
Influence of particles size	150-180	60	17.5
	180-250		
	> 250		

The influence of magnetization of the composite materials in their mechanical properties was also studied, a classical induction method was used to obtain the remnant magnetization of the composites after being submitted to an applied magnetic field of 1 T in the longitudinal direction of the sample magnetizing it in this direction. The measurements were obtained by means of a fluxmeter integrator EF4 (Magnet Physik) connected to a pick up coil that surrounds the composite. This coil of 7 mm inner diameter consists of 20 000 turns of copper wire of 0.05 mm diameter.

Instrumented microindentation (P-h curves, scheme presented in Figure 1 is implemented to characterize the micro-mechanical behavior of the obtained composite materials. Loading-unloading tests were carried out by load and displacement control in order to evaluate pseudo-creep phenomena (viscoelasticity) and stress relaxation, respectively. These tests were performed in a Microtest machine (MTR3/50-50/NI) using a Vickers indenter. Figure 2 shows the experimental details of performed tests. At least three measurements were performed for each test condition and composite material.

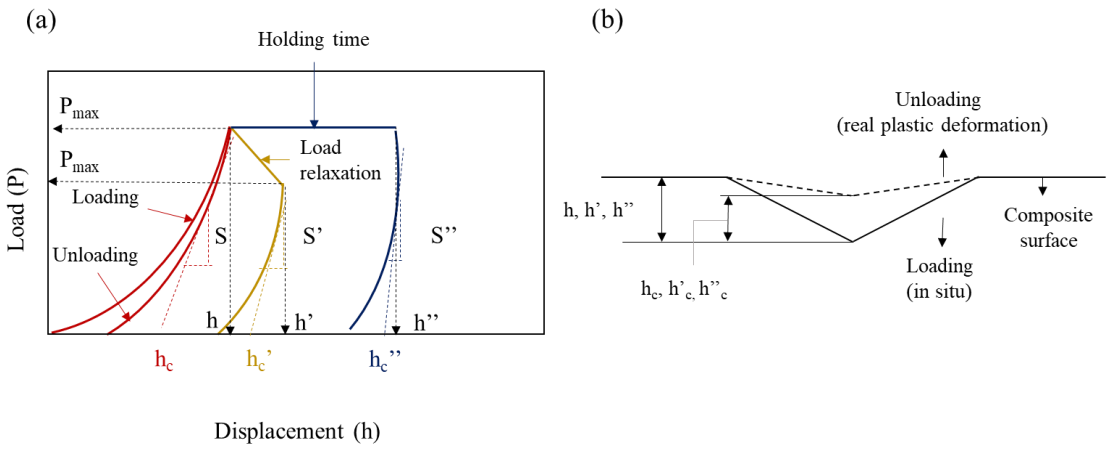

Figure 1. Scheme of instrumented microindentation tests: (a) conventional P-h curve (in red), pseudo-creep behavior (load control) (in blue) and stress relaxation (displacement control) (in yellow) and (b) indentation geometry during loading and unloading.

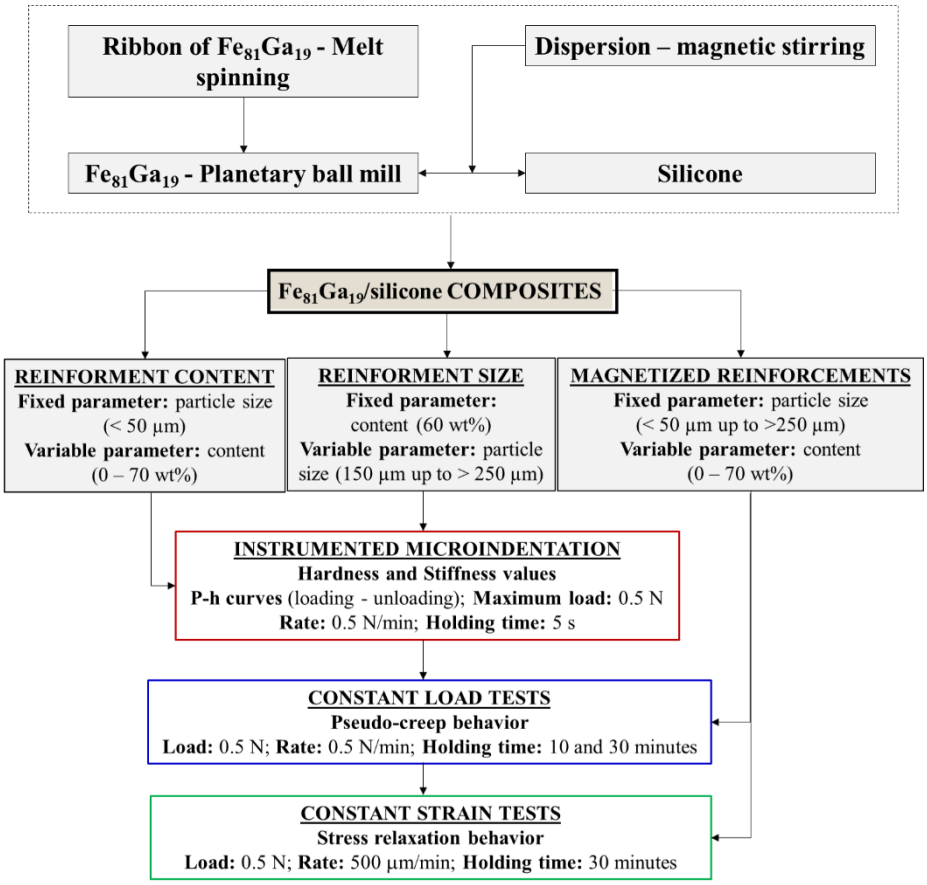

Figure 2. Outline of the experimental procedures for manufacturing and micro-mechanical characterization of the studied $Fe_{81}Ga_{19}$/silicone composites.

The hardness and the Young´s modulus were calculated from the resulting loading-unloading curves by using the Oliver and Pharr method [20-23] and corrections were made taking into account changes induced to the indenter geometry due to wear or damage because of the use. Based on Oliver and Pharr method, Hardness (H) was calculated following the equation (1):

$$H = \frac{P_{max}}{A} \quad (1)$$

where P_{max} is the maximum load and A is the contact area calculated from the depth of contact between the indenter and the sample surface, h_c (h_c' and h_c'' for stress relaxation and pseudo-creep tests, respectively). The effective elastic modulus (E_{eff}), which takes

(2)

into account elastic displacements in both, the indenter and the sample, was calculated using equation (2):

$$E_{eff} = \frac{S}{\beta \frac{2}{\sqrt{\pi}} \sqrt{A}} \quad (2)$$

where S is the slope of unloading P-h curve (S' and S'' for stress relaxation and pseudo-creep tests, respectively) and β is a correction factor dependent on the indenter. The elastic modulus was then calculated from E_{eff} considering the elastic modulus (E_i) and the Poisson's ratio of the indenter (ν_i) and the one of the silicone (ν) following the equation (3):

$$E = \frac{(1 - \nu^2)}{1/E_{eff} - (1 - \nu_i^2)/E_i} \quad (3)$$

3. Results and discussion

In this section, results related to the micro-mechanical behavior of $Fe_{81}Ga_{19}$/silicone composite materials are discussed. The Young's modulus and Vickers micro-hardness were evaluated to elucidate the influence of: **1)** weight fraction of the metallic reinforcement, **2)** reinforcement particles size and **3)** magnetization of $Fe_{81}Ga_{19}$ soft magnetic particles. In this context, considering the properties of the polymeric matrix of the studied composite materials, pseudo-creep behavior (viscoelasticity) and stress relaxation were also evaluated.

3.1. Influence of reinforcement content

The incorporation of $Fe_{81}Ga_{19}$ microparticles into the silicone matrix can modified the mechanical properties of the composites. One important parameter is the filler content. Figure 3a and 3b shows optical micrographs of composites reinforced with contents of

60 wt%, a good dispersion and integration of the filler into the silicone matrix is achieved. As it can be seen in Figure 3b, the interphase between the filler and the silicone has continuity as the silicone evolves the particles and wet the surface. In order to analyze the influence of the $Fe_{81}Ga_{19}$ content in micro-mechanical properties of the proposed composites, Figure 3c shows P-h loading and unloading curves for the silicone and composites reinforced with 50, 60 and 70 wt% of particles with a size < 50 μm [24]. On the other hand, the values of calculated hardness and elastic modulus as a function of the filler content are graphed in Figure 3d. Table 2 shows the results associated to the micro-indentation behavior.

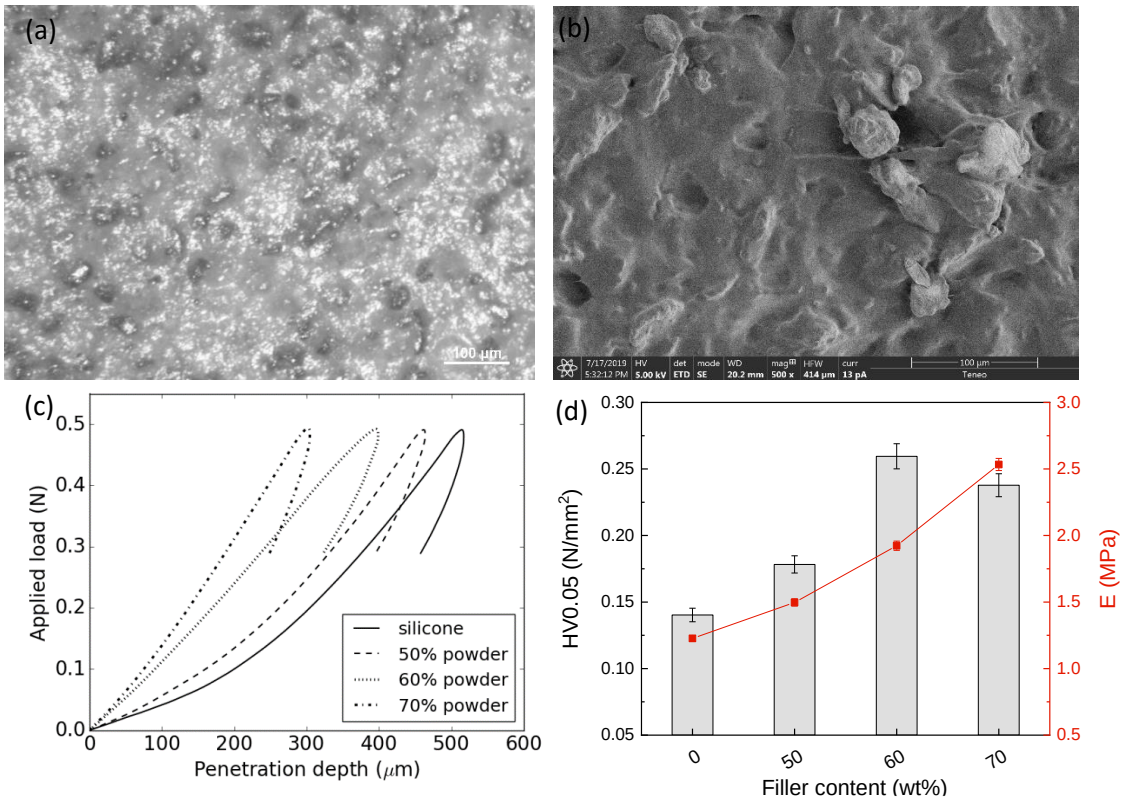

Figure 3. Influence of $Fe_{81}Ga_{19}$ particle wt% content in micro-mechanical behavior of composites studied: (a) optical and (b) SEM micrographs of 60 wt% reinforced composite, (c) loading-unloading curves, and (d) Young's modulus and micro-hardness estimated value. Note: range of reinforcement particle size is constant (<50 μm).

Table 2. Parameters characteristic of P-h curve and micro-mechanical (Young's modulus and micro-hardness) values of composites with different $Fe_{81}Ga_{19}$ reinforcement wt% content. **Note:** the elastic recovery has been evaluated during unloading at 0.3 N.

Composites		h (μm)	Elastic Recovery		HV0.05 (N/mm^2) ($x \cdot 10^{-1}$)	Elastic Modulus (MPa)
Matrix	Reinforcements - $Fe_{81}Ga_{19}$ powder Content (wt%)		Absolut (μm)	Relative (%)		
Silicone	0	515	52	10	1.40 ± 0.05	1.23 ± 0.02
	50	462	61	13	1.78 ± 0.06	1.48 ± 0.03
	60	396	67	17	2.60 ± 0.09	1.92 ± 0.03
	70	302	49	16	2.28 ± 0.01	2.53 ± 0.05

As it was expected, generally, an increment in the weight content of reinforcement induces an enhancement of the stiffness, micro-hardness (the maximum depth penetration diminishes) and the elastic recovery (absolute and relative) of the composite materials [25]. The hardness of the particles used as reinforcement is higher than that of the silicone matrix. Additionally, the average interparticle distance diminishes by increasing the filler content (Figure 3a and 3b) [26]. For this reason, the constrain of the polymeric matrix is more pronounced with the increment of the filler content and, consequently, plastic strain is limited, causing the increment of the properties mentioned above [27]. On the other hand, deeper studies should be carried out in order to completely characterize the influence in micro-mechanical behavior of: 1) the quality of the reinforcement/matrix interphase [28], which is going to condition the efficiency of load transfer and 2) the steric phenomena due to the addition of the fillers.

3.2. Influence of particles size

Another important parameter influencing the micro-mechanical properties of $Fe_{81}Ga_{19}$/silicone composite materials is the particle size of the reinforcement, Figure 4a and 4b shows optical images of composites reinforced with particles sizes of

150-180 and > 250 µm. Generally, particles with a bigger size are less effective increasing the micro-hardness and the Young's modulus. J. Choi et al. [29] and S. Yu et al. [30] has reported that this tendency is due to the thickness of the interphase between the microparticles and the polymeric matrix, named adsorption layer, where the polymeric chains mobility is limited. In order to elucidate the influence in this particular case, Figure 4c shows P-h loading and unloading curves for composites reinforced with 60 wt% and different particles size ranges: 150 – 180 µm, 180 - 250 µm and bigger than 250 µm and Table 3 shows characteristic parameters of micro-indentation behavior [31]. Additionally, the values of calculated micro-hardness and elastic modulus as a function of the particle size are plotted in Figure 4d and also included in Table 3. From obtained results, it can be seen that the maximum micro-hardness and Young's modulus were obtained for composites reinforced with a particle size range of 150 – 180 µm, inducing and enhancement of more than 5 times of the micro-hardness of the silicone and more than twice in the case of the Young's modulus. It is important to point out that the maximum depth penetration of composite materials reinforced with a 60 wt% and a size distribution of <50 µm for the same load was less than 200 µm, which supports the observed tendency. A bigger size of particles makes that the effective number of particles incorporated into the matrix for a same weight content lower (Figure 4a and 4b) [32]. Consequently, the number of blocking centers contributing to the steric phenomena is lower and, then, the polymeric chains have higher mobility because of a lower mechanical interlocking [33,34]. This fact and the reduction of the specific surface area of the reinforcement, which leads to a less contact surface between the filler and the silicone matrix, provokes the tendency observed: particles with bigger sizes are less effective to increase the micro-hardness and Young's modulus of silicone.

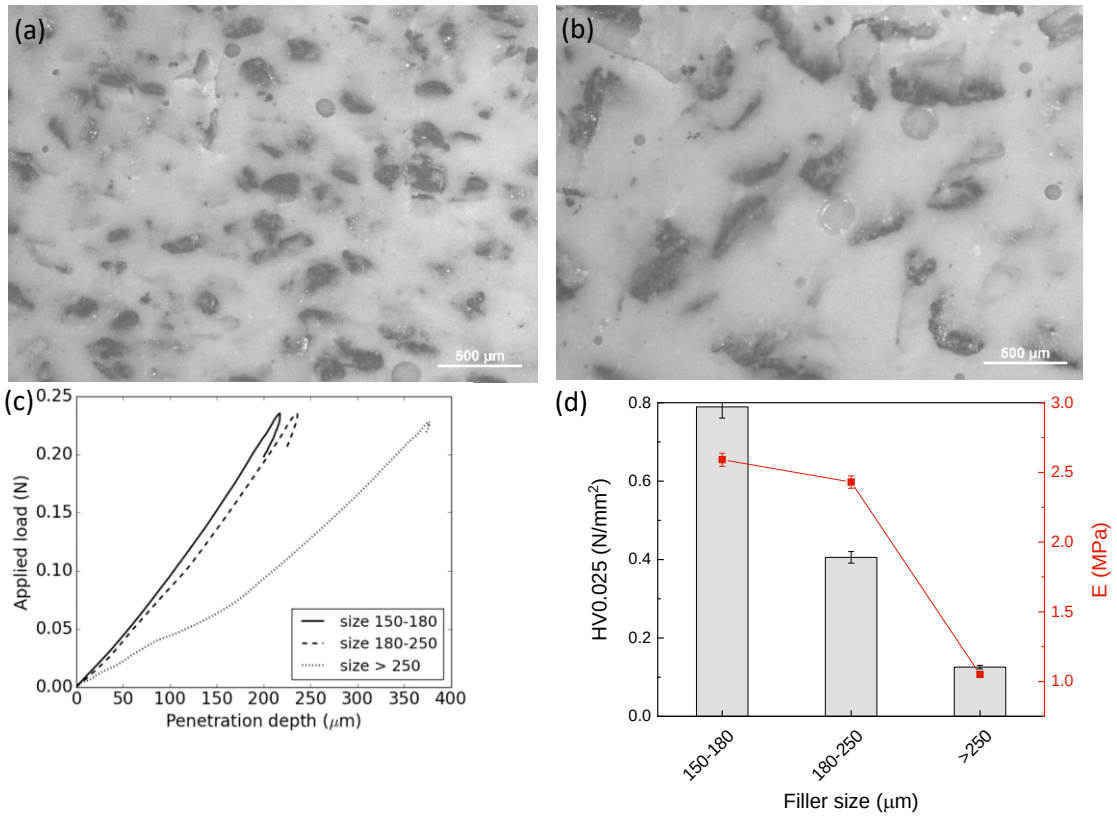

Figure 4. Influence of $Fe_{81}Ga_{19}$ particle size: optical micrographs of composites reinforced with particles size of (a) 150-180 and (b) > 250 µm, (c) P-h curves (holding time: 5 s) and (d) micro-mechanical properties. Note: in this case, we used a 60 wt% of $Fe_{81}Ga_{19}$.

Table 3. Parameters of the loading-unloading behaviour for composites reinforced with 60 wt% and different range of particle sizes studied. **Note:** the elastic recovery has been evaluated during unloading at 0.2 N.

Composites		h (µm)	Elastic Recovery		HV0.025 (N/mm^2) (x 10^{-1})	Elastic Modulus (MPa)
Matrix	Reinforcements - $Fe_{81}Ga_{19}$ powder Particles size (µm)		Absolut (µm)	Relative (%)		
Silicone	150-180	217	4	1.9	7.9 ± 3	2.59 ± 0.05
	180-250	235	4	1.7	4.1 ± 1	2.43 ± 0.04
	> 250	376	2	0.5	1.26 ± 0.05	1.05 ± 0.02

The results included in Table 3 also supports the previous discussion, the maximum penetration depth in composites reinforced with particles in the range of 150 – 180 µm was considerably lower than in composites filled with particles sizes between 180 – 250 µm and > 250 µm. This is caused because of a higher effectiveness of constrain of

polymeric chains mobility due to the incorporation of a higher number of particles with higher specific surface area, which was mentioned above.

3.3. Influence of test conditions: control load and strain

The influence of the strain rate, type and holding time of the mechanical solicitation on the mechanical behavior of the composite materials are well known, particularly it is significant in polymer matrix composites materials. In this context, viscoelasticity phenomena (pseudo-creep) and stress relaxation become important in-service performance of this composite materials [35]. The influence of holding time in the mechanical behavior of a selection of the studied materials is shown in Figure 5 and Table 4. These results make possible to confirm the following relevant ideas: **1)** a clear pseudo-creep behavior is observed in the silicone matrix and the evaluated composite materials, i.e. significant increment of the penetration depth is observed for longer maintained constant load (plateau), **2)** viscoelasticity phenomenon is dependent on the metallic reinforcement ($Fe_{81}Ga_{19}$) content and size distribution, being this effect more representative when the content increases and/or the particles size diminishes [36]. This fact could be related to the failure of the weak interfaces matrix/reinforcement when they are subjected to a constant stress enduring in time (micro-cavities coalescence); **3)** micro-hardness and stiffness diminish with the holding time, independently on the reinforcement content and size distribution. The failure of the interfaces diminishes the contribution of the particles as obstacles to the movement of polymeric chains during strain; and, **4)** in general, the elastic recovery is also dependent on the holding time, this diminution could be associated to the slipped polymeric chains, which cannot return to the initial position once the mechanical load ceases.

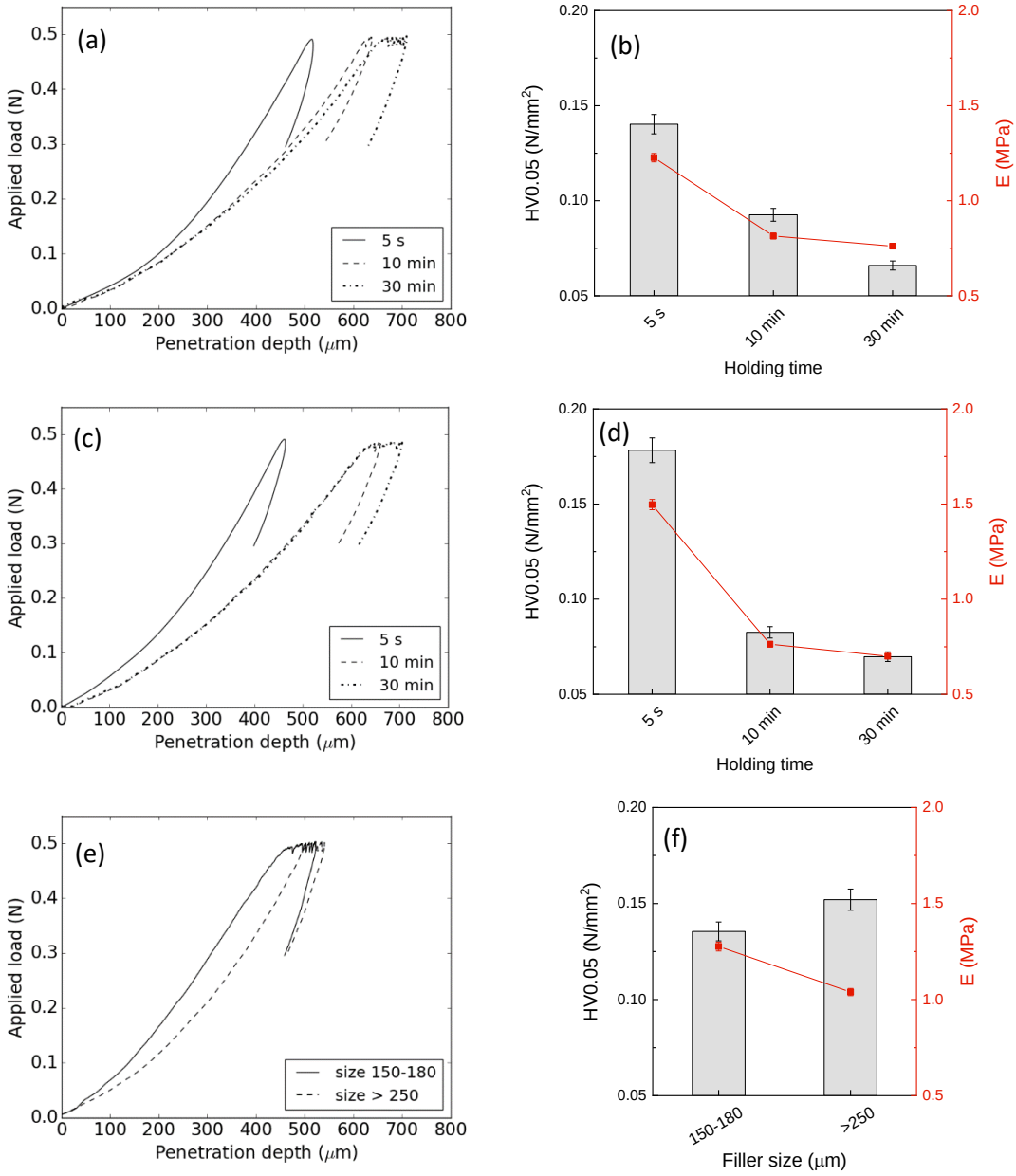

Figure 5. Influence of the holding time and $Fe_{81}Ga_{19}$ particles characteristic (wt% and ranges of size) in the pseudo-creep and micro-mechanical (stiffness and hardness) behavior: (a, b) silicone matrix, (c, d) composite with 50%wt $Fe_{81}Ga_{19}$ (reinforcement size <50 μm); and (e, f) silicone with 60 wt% of particles (two $Fe_{81}Ga_{19}$ powder size).

Table 4. Pseudo-creep behaviour for composites studied at different holding time: influence of reinforcements wt% and size.

Composites						Elastic Recovery			
Matrix	Reinforcements - $Fe_{81}Ga_{19}$ powder		Holding times (min)	h'' (μm)	Pseudo-creep (μm)	Absolut (μm)	Relative (%)	HV0.05 (N/mm^2) (x 10^{-1})	Elastic Modulus (MPa)
	Content (wt%)	Particles size (μm)							
Silicone	0	< 50	10	625	13	95	15	0.93 ± 0.05	0.81 ± 0.01
			30	670	39	79	11	0.66 ± 0.03	0.76 ± 0.01
	50		10	628	32	89	14	0.83 ± 0.03	0.76 ± 0.01
			30	627	78	91	13	0.70 ± 0.03	0.70 ± 0.01
	60	150-180	30	474	49	65	12	1.35 ± 0.05	1.28 ± 0.02
		> 250	30	515	25	78	15	1.52 ± 0.05	1.04 ± 0.02

On the other hand, Figure 6 and Table 5 shows the composites behavior under constant strain conditions. The analysis of the results clearly elucidated the presence of stress relaxation phenomena (note the applied load drop and the values of the different relaxation times) [37, 38], which depend on the metallic reinforcement content and size distribution, as well as on the time the associated constant strain for each material when a load of 1 N is applied. In terms of the relaxation time, the highest values were obtained for the silicone matrix compared to the composite materials compared and they were lower as the particles content increased and the size distribution was smaller, which is in accordance with tendencies observed in the micro-mechanical properties explained before.

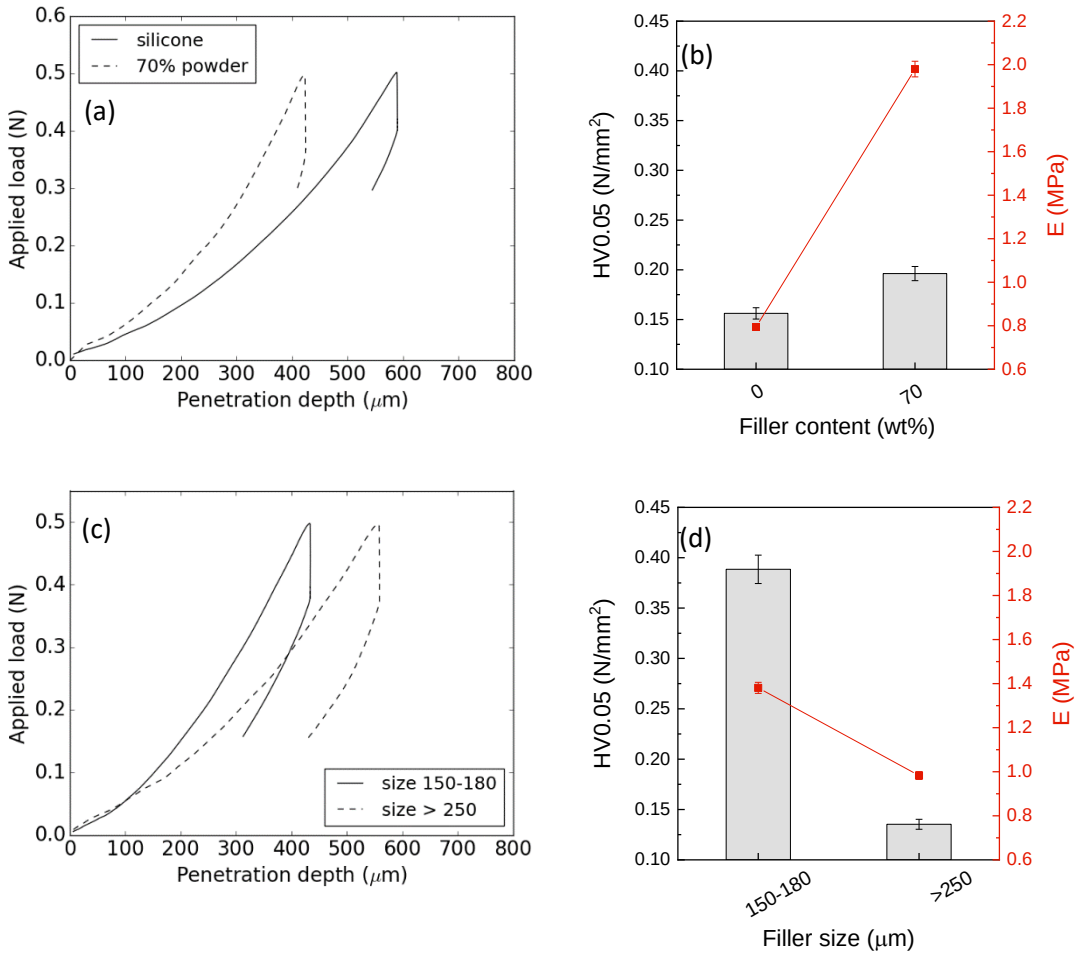

Figure 6. Stress relaxation behavior for the composites with 60 wt % $Fe_{81}Ga_{19}$ for different reinforcement content (for silicone and silicone with 70% $Fe_{81}Ga_{19}$ powder < 50 μm) and sizes of particles: (a) loading-unloading curves and (b) mechanical properties. Note: the stationary strain in each case (associated to a load of 1 N) was hold for 30 minutes.

Table 5. Stress relaxation behavior and mechanical properties.

Composites							
Matrix	Reinforcements - $Fe_{81}Ga_{19}$ powder		Load Drop		τ* (min)	HV0.05 (N/mm^2) (x 10^{-1})	Elastic Modulus (MPa)
	Content (wt%)	Particles size (μm)	Absolut (N)	Relative (%)			
Silicone	0	<50	0.105	21	135	1.56 ± 0.06	0.79 ± 0.01
	70		0.151	30	89	1.96 ± 0.07	1.98 ± 0.04
	60	150-180	0.123	25	109	3.9 ± 0.1	1.38 ± 0.03
		> 250	0.134	27	100	1.35 ± 0.05	0.98 ± 0.02

* τ: relaxation time calculated from: $\sigma = \sigma_0 + e^{-\tau/t}$, where σ is the load after relaxation, σ_0 is the initial load and t the time the initial load is hold.

3.4. Influence of magnetization on micromechanical behaviour

The hysteresis loops of the initial powders are shown in Figure 7 and their magnetic characteristics in Table 6. As can be observed, the magnetic saturation (Ms), of the powders does not change with the mechanical milling meanwhile the coercivity (Hc), and the remnant magnetization (Mr), change with the particle size. The Hc is an important identification factor of the soft magnetic behavior of the material and in our case the maximum value is 58 Oe, indicating that all the powders have a soft magnetic behavior.

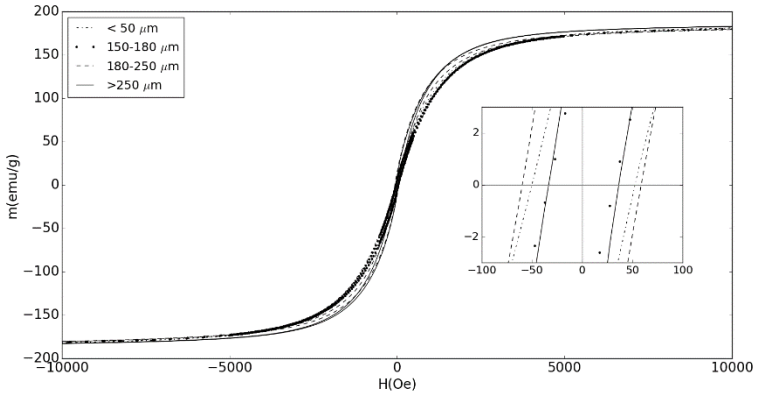

Figure 7. Magnetic hysteresis loops of the powders. The inset shows a zoom of the central part of the hysteresis loops.

Table 6. Magnetic characteristics of the initial powders.

Size of the powder (μm)	Ms (emu/g)	Hc (Oe)	Mr (emu/g)
< 50	183.9 ± 0.2	52 ± 1	8.73 ± 0.15
150-180	183.0 ± 0.2	32 ± 1	6.23 ± 0.15
180-250	182.4 ± 0.2	58 ± 1	12.87 ± 0.15
> 250	184.8 ± 0.2	33 ± 1	9.80 ± 0.15

On the other hand, the Table 7 shows and increase of the Mr, as the metallic reinforcement content and size increase over the studied composites.

Table 7. Remnant magnetization of the composites.

Size of the powder (μm)	% of powder	Remnant Magnetization (G)
< 50	50	20.7 ± 0.5
	60	41.4 ± 0.5
	70	63.4 ± 0.5
150-180	60	39.2 ± 0.5
180-250		50.3 ± 0.5
> 250		65.6 ± 0.5

Results of micromechanical behavior of composite materials before and after being subjected to a magnetic field of 1 T, elucidate, generally: **1)** an increment of the plastic strain phenomena (pseudo-creep), as seen in Figure 8 and 9 and Table 8 when composite materials are magnetized, being directly proportional to the remnant magnetization values, and **2)** the micro-hardness and stiffness of the reinforced materials increase. Nevertheless, different tendencies were observed in composite materials with high remnant magnetization (63-66 G), showing a diminution of micro-mechanical properties. In samples reinforced with 70 wt% $Fe_{81}Ga_{19}$, which showed a remnant magnetization of 63.4 ± 0.5 G, the stiffness diminishes with magnetization. Additionally, in samples reinforced with particles bigger than 250 μm, with a remnant magnetization of 65.6 ± 0.5 G, micro-hardness decreased with magnetization.

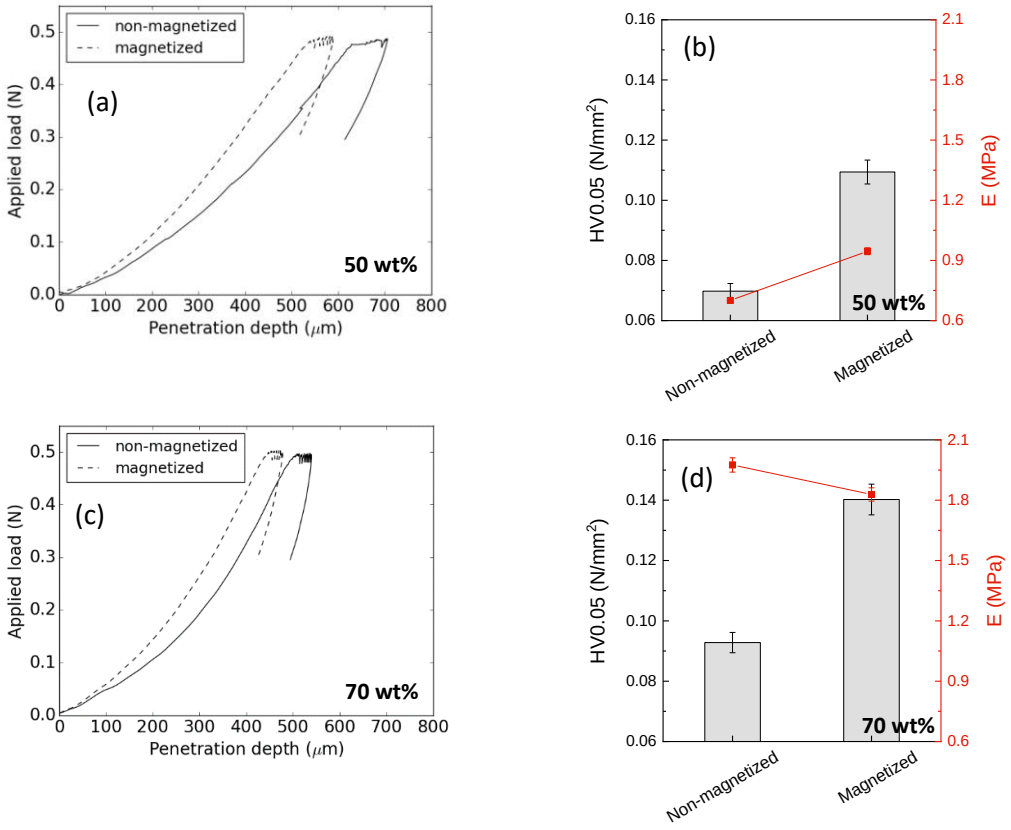

Figure 8. Pseudo-creep behavior for 30 min holding time (a, b) silicone with 50% $Fe_{81}Ga_{19}$ powder and (c, d) silicone with 70% $Fe_{81}Ga_{19}$ powder: (a, c) loading-unloading curves and (b, d) mechanical properties.

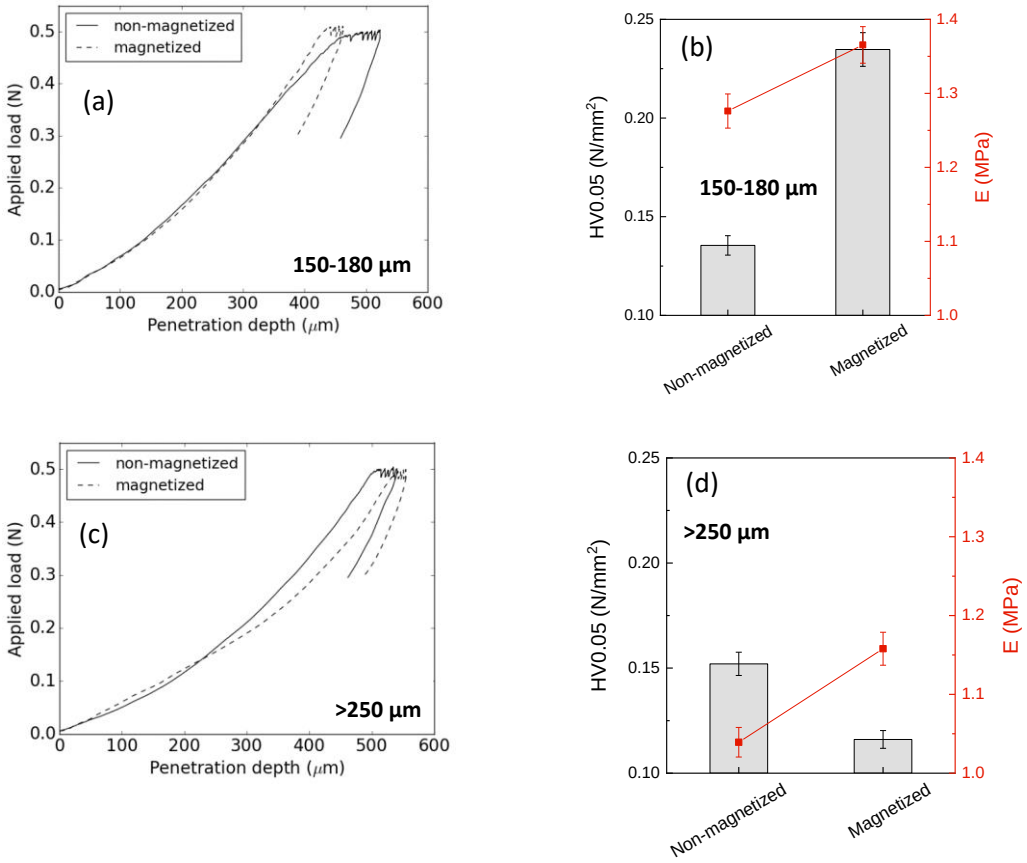

Figure 9. Pseudo-creep behavior (30 min holding time) for the composites with 60 wt % $Fe_{81}Ga_{19}$ (a, b) particles size 150-180 μm and (c, d) particles size >250 μm: (a, c) loading-unloading curves and (b, d) mechanical properties.

Table 8. Pseudo-creep behavior (30 min holding time) for non-magnetized and magnetized samples.

Composites						Elastic Recovery			
Matrix	Reinforcements - $Fe_{81}Ga_{19}$ powder		Magnetic state - Remnant magnetization (G)	h'' (μm)	Pseudo-creep (μm)	Absolut (μm)	Relative (%)	HV0.05 (N/mm^2) (x 10^{-1})	Elastic Modulus (MPa)
	Content (wt%)	Particles size (μm)							
Silicone	50	<50	Non-magnetized	627	0.70 ± 0.03	91	13	0.70 ± 0.03	0.70 ± 0.01
			20.7	548	1.09 ± 0.04	75	13	1.09 ± 0.04	0.95 ± 0.02
	70		Non-magnetized	512	0.93 ± 0.03	46	9	0.93 ± 0.03	1.98 ± 0.04
			63.4	454	1.40 ± 0.05	55	11	1.40 ± 0.05	1.83 ± 0.03
	60	150-180	Non-magnetized	474	1.35 ± 0.05	65	12	1.35 ± 0.05	1.28 ± 0.02
			39.2	442	2.35 ± 0.08	76	16	2.35 ± 0.08	1.37 ± 0.02
		> 250	Non-magnetized	515	1.52 ± 0.06	78	15	1.52 ± 0.06	1.04 ± 0.02
			65.6	537	1.16 ± 0.04	69	12	1.12 ± 0.04	1.16 ± 0.02

4. Conclusions.

The micro-mechanical behavior and magnetization of $Fe_{81}Ga_{19}$/silicone composite materials reinforced with different filler contents and size distributions were analyzed. It was corroborated that the micro-hardness, stiffness and elastic recovery of the studied composite materials increased with the filler content up to a weight fraction of 60 wt%. When 70 wt% of $Fe_{81}Ga_{19}$ was incorporated, the elastic modulus stabilizes as a higher stiffness was not achieved but an increase in micro-hardness was observed. It was also observed that an increase in particles size distribution caused a detriment in micromechanical properties, i.e. micro-hardness, stiffness and elastic recovery due to a lower specific surface area which makes the load transfer less efficient, being more significant for particles sizes >250 µm. Pseudo-creep behavior was also dependent on $Fe_{81}Ga_{19}$ content and size distribution. A reduction in the filler content as well as an augment of the particles size distribution induced a diminution in pseudo-creep of composite materials. Additionally, a higher filler content and particle size distribution caused the lowering of the relaxation time and higher relaxation in composite materials. In terms of magnetic behavior, the addition of higher $Fe_{81}Ga_{19}$ content and size distribution provokes an increase in the remnant magnetization. As a consequence of the remnant magnetization in composite materials, micro-mechanical properties changes, experiencing an increase in all cases but when a size distribution >250 µm was used. As a final conclusion, the composite materials that showed the best behavior related to both micro-mechanical and magnetic properties were the ones with a 60 wt% and a size distribution of 150 – 180 µm and 70 wt% with a particle size < 50 µm.

Acknowledgements

This work was supported in part by the Principality of Asturias Government under grant GRUPIN 14-037. The authors are grateful to the technicians Dr. D. Martínez of the Scientific Services of the University of Oviedo and J. Pinto of Materials laboratory of the University of Seville for the assistance in mechanical characterization. Finally, also to Professor Victorino Franco for his collaboration in magnetic measurements.

References.

[1] P.H.C. Camargo, K.G. Satyanarayana, F. Wypych, Nanocomposites: synthesis, structure, properties and new application opportunities. Mat. Res. 12 (2009) 1-39. http://dx.doi.org/10.1590/S1516-14392009000100002

[2] D. Neupane, M. Ghimire, H. Adhikari, A. Lisfi, S.R.Mishra, Synthesis and magnetic study of magnetically hard-soft $SiFe_{12-y}Al_yO_{19}$-x wt%$Ni_{0.5}Zr_{0.5}Fe_2O_4$ nanoomposites. AIP Adv. 7 (2017) 055602. https://doi.org/10.1063/1.4978398

[3] E. Dragasius, Z. Korobko, Z. Novikava, E. Sermyazhko, Magnetosensitive polymer composites and effect of magnetic field directivity on their properties. Sol. St. Phen. 251 (2016) 3-7. https://doi.org/10.4028/www.scientific.net/SSP.251.3

[4] M. kukla, J. Górecki, I. Malyda, K. Taláska, P. Tarkowski, Determination of mechanical properties of magnetorheological elastomers (MRES). Procedia Eng. 177 (2017)324-330. https://doi.org/10.1016/j.proeng.2017.02.233

[5] P. Song, T-J. Peng, Y-L. Yue, H. Zhang, Z. Zhang, Y-C Fan, Mechanical properties of silicone composites reinforced with micron-and nano-sized magnetic particles. Express Poly. Lett. 7 (2013) 546-553. https://doi.org/10.3144/expresspolymlett.2013.51

[6] P. H. C. Camargo; K. G. Satyanarayana, F. Wypych, Magnetosensitive polymer composite and effect of magnetic field directivity on their properties. Mat. Res. 12 (2009) 1-39. http://dx.doi.org/10.1590/S1516-14392009000100002

[7] R. Elhajjar, C.T. Law, A. Pegoretti, Magnetostrictive polymer composites: Recent advances in materials, structures and properties. Prog Mater Sci. 97 (2018) 204-229. https://doi.org/10.1016/j.pmatsci.2018.02.005

[8] L. K. Lagorce, M. G. Allen, Magnetic and Mechanical Properties of Micromachined Strontium Ferrite/Polyimide Composites. J. Microelectromech. S. 6 (1997) 307-312. https://doi.org/ 10.1109/84.650127

[9] G. Andrei, D. Dinia, l. Andrei, J. Optoelectron. Lightweight magnetic composites for aircraft application. Adv. M. 8 (2006) 726-730.

[10] M. L. Tupper, P. E. Fabian, F. L. Beavers, Reducing the risk of insulating magnets. IEEE Trans. Appl. Supercond 10 (2000) 1350-1353. https://doi.org/10.1109/77.828487

[11] G. Riesgo, J. Carrizo, L. Elbaile, R.D. Crespo, R. Sepúlveda, J.A. García, Magnetostrictive properties of FeAl/polyester and FeAl/silicone composites. Mater. Sci. Eng. B, 215 (2017) 56-63. https://doi.org/10.1016/j.mseb.2016.11.004

[12] G.Y. Thou, Z.Y. Jiang, Deformation in magnetorheological elastomer and elastomer-ferromagnet composite driven by a magnetic field. Smart. Mater. Struct. 13 (2004) 309-316. https://iopscience.iop.org/article/10.1088/0964-1726/13/2/009

[13] I. Borcea, O. Bruno, On the magneto-elastic properties of elastomer-ferromagnet composites. J. Mech. Phys. Solids. 49 (2001) 2877-919. https://doi.org/10.1016/S0022-5096(01)00108-9

[14] G.V. Stepanov, S.S. Abramchuck, D.A. grishin, L.V. Nikitin, E.-Yu kramaranko, A.R. Khoklov, Effect of a homogeneous magnetic field on the viscoelastic behavior of magnetic elastomers. Polymer 48 (2007) 488-495. https://doi.org/10.1016/j.polymer.2006.11.044

[15] M. Lokander, B. Stenberg, Improving the magnetorheological effect in isotropic magnetorheological rubber materials. Polym. Test. 22 (2003) 677-680. https://doi.org/10.1016/S0142-9418(02)00175-7

[16] G.V. Stepanov, A.V. Chertonich, E.Yu Kramanenko, Magnetorheological and deformation properties of magnetically controlled elastomers with hard magnetic filler. J. Magn. Magn. Mater. 324 (2012) 3448-3451. https://doi.org/10.1016/j.jmmm.2012.02.062

[17] J.-Hoi Koo, A. Dawson, H.-Jo Jung, Characterization of actuation properties of magnetorhelogical elastomers with embedded hard magnetic particles. J. Intell. Mater. Syst. Struct., 23 (2012) 1049-1054. https://doi.org/10.1177/1045389X12439635

[18] E. Yu Kramarenko, A.V. Chertovich, G.V. Stepanov, A.S. Semisalova, L.A. Makarova, N.S. Peov, A.R. Khokhlov, Magnetic and viscoelastic response of

elastomers with hard magnetic filler. Smart. Mater. Struct. 24 (2015) 035002. https://iopscience.iop.org/article/10.1088/0964-1726/24/3/035002

[19] L.A. Makarova, Y.A. Alekhina, N.S. Perov, Peculiarities of magnetic properties of magnetoactive elastomers with hard magnetic filler in crossed magnetic fields. J. Magn. Magn Mater. 440 (2017) 30–32. https://doi.org/10.1016/j.jmmm.2016.12.095

[20] W.C. Oliver, G.M. Pharr, Measurement of hardness and elastic modulus by instrumented indentation: Advances in understanding and refinements to methodology. J. Mater. Res. 2004;19:3–20. https://doi.org/10.1557/jmr.2004.19.1.3

[21] D.S. Harding, W.C. Oliver, G.M. Pharr, S.P. Baker, P. Børgesen, P.H. Townsend, C.A. Ross, C.A. Volkert, Thin films: Stresses and mechanical properties. V. MRS Sympos. Proc. Vol. 356. 1995. https://doi.org/10.1533/9780857096296.2.353

[22] I.N. Sneddon, The relation between load and penetration in the axisymmetric Boussinesq problem for a punch of arbitrary profile. Int. J. Eng. Sci. 1965;3:47–57. https://doi.org/10.1016/0020-7225(65)90019-4

[23] W.C. Oliver, G.M. Pharr, An improved technique for determining hardness and elastic modulus using load and displacement sensing indentation experiments. J. Mater. Res. 1992;7:1564–1583. https://doi.org/10.1557/JMR.1992.1564

[24] R.F. Gibson, A review of recent research on nanoindentation of polymer composites and their constituents. Compos. Sci. Technol. 105 (2014) 51–65. https://doi.org/10.1016/j.compscitech.2014.09.016

[25] Y. Yana, M. Pottsa, Z. Jianga, V. Sencadas, Synthesis of highly-stretchable graphene – poly(glycerol sebacate) elastomeric nanocomposites piezoresistive sensors for human motion detection applications. Compos. Sci. Technol. 162 (2018) 14-22. https://doi.org/10.1016/j.compscitech.2018.04.010

[26] B. H. Rutz, J. C. Berg, A review of the feasibility of lightening structural polymeric composites with voids without compromising mechanical properties. Adv. Colloid. Interfac. 160 (2010) 56-75. https://doi.org/10.1016/j.cis.2010.07.005

[27] A. A. Ashor, M. M. Vuksanović, N. Z. Tomić, A. Marinković, R. J. Heinemann, The influence of alumina particle modification on the adhesion of the polyacrylate matrix composite films and the metal substrate. Compos. Interface 26 (2019) 417-430. https://doi.org/10.1080/09276440.2018.1506240

[28] S. Chouhan, A. K. Bajpai, R. Bhatt, Analysis of topographical parameters and interfacial interaction of zinc oxide reinforced poly (vinyl alcohol-g-acrylonitrile)

nanocomposite film surfaces using atomic force microscopy. Nano-Structures & Nano-Objects 18 (2019) 100308. https://doi.org/10.1016/j.nanoso.2019.100308

[29] A. Flores, F. Ania, F.J. Baltá-Calleja, From the glassy state to ordered polymer structures: A microhardness study. Polymer 50 (2009) 729–746. https://doi.org/10.1016/j.polymer.2008.11.037

[30] A.M. Díez-Pascual, M.A. Gómez-Fatou, F. Ania, A. Flores, Nanoindentation in polymer nanocomposites. Prog. Mater. Sci. 67 (2015) 1–94. https://doi.org/10.1016/j.pmatsci.2014.06.002

[31] H. Takagi, M. Fujiwara, Set of conversion coefficients for extracting uniaxial creep data from pseudo-steady indentation creep test results. Mater. Sci. Eng. A 602 (2014) 98–104. https://doi.org/10.1016/j.msea.2014.02.060

[32] S. Botsi, C. Tsamis, M. Chatzichristidi, G. Papageorgiou, E. Makarona, Facile and cost-efficient development of PMMA-based nanocomposites with custom-made hydrothermally-synthesized ZnO nanofillers. Nano-Structures & Nano-Objects 17 (2019) 7-20. https://doi.org/10.1016/j.nanoso.2018.10.003

[33] P. Katti, K.V. Kundan, S. Kumar, S. Bose, Improved mechanical properties through engineering the interface by poly (ether ether ketone) grafted graphene oxide in epoxy based nanocomposites. Polymer 122 (2017) 184-193. https://doi.org/10.1016/j.polymer.2017.06.059

[34] S. Thomas, K. Joseph, S. K. Malhotra, K. Goda, M. S. Sreekala, Polymer Composites, Nanocomposites 1st Edition, Wiley-VCH.

[35] J. Liu, P. Lin, X. Li, S.Q. Wang, Nonlinear stress relaxation behavior of ductile polymer glasses from large extension and compression. Polymer 81 (2015) 129-139. https://doi.org/10.1016/j.polymer.2015.11.015

[36] N. Obaid, M.T. Kortschot, M. Sain, Compos. Predicting the stress relaxation behavior of glass-fiber reinforced polypropylene composites. Sci. Technol. 161 (2018) 85-91. https://doi.org/10.1016/j.compscitech.2018.04.004